THE JOURNAL OF PHYSICAL CHEMISTRY C

Article

pubs.acs.org/JPCC

Oxidation of Gold Nanoparticles by Au(III) Complexes in Toluene

Paul J. G. Goulet,*,† Agustina Leonardi, and R. Bruce Lennox*

Department of Chemistry and Centre for Self-Assembled Chemical Structures (CSACS), McGill University, 801 Sherbrooke Street West, Montreal, Quebec, Canada, H3A 2K6

Supporting Information

ABSTRACT: The rapid, stoichiometric oxidation of gold nanoparticles by tetraalkylammonium and tetraalkylphosphonium Au(III) complexes in toluene is reported here. Nanoparticle oxidation proceeds via a comproportionation mechanism and generates stable Au(I) complexes of the ammonium and phosphonium cations used. These reactions are studied for several organo-soluble nanoparticle systems, employing different cations and halides in the Au(III) oxidant complex, and a mechanism for the comproportionation reaction is proposed. It is demonstrated that Au nanorods stabilized in toluene can be progressively "sculpted" by Au(III) complexes. Measurement artifacts caused by the reduction of Au(I) and Au(III) species during conventional TEM imaging are also demonstrated and discussed. The results presented here provide insight into a host of issues in the chemistry of Au nanoparticles: nanoparticle oxidation, reduction of Au(III) species to Au(0) nanoparticles, galvanic replacement reactions using Au(III), and sample changes induced by TEM imaging. The oxidation of Au nanoparticles by Au(III) complexes in nonpolar solvents is expected to be a valuable new tool for nanoparticle sculpting, dissolution of nanogold templates, Au content determination, ligand removal from nanoparticles, nanoparticle purification, and Au recovery processes.

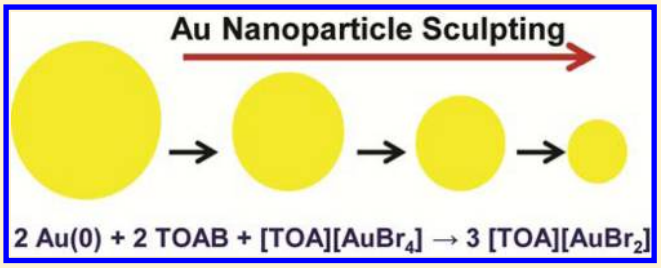

INTRODUCTION

Gold nanoparticles are among the most studied and utilized materials in nanoscience and nanotechnology. They are produced in a wide range of shapes and sizes and can be broadly functionalized through their ligand shell.[1−4] They are employed in numerous applications including those in catalysis, sensing, imaging, diagnostics, therapy, and delivery.[2,3,5−7] The well-known nobility and associated biocompatibility of gold make it a particularly attractive metal for use on the nanoscale, especially for biomedical applications.[3,5,7] Under certain conditions, however, nanoscale gold can be quite reactive. These reactions have important implications for the formation, growth, transformation, structure, stability, reactivity, and functionalization of gold nanoparticles.[8] They also likely play an important role in determining the toxicity and catalytic activity of these nanomaterials.

Perhaps the most important reaction of Au(0) is its dissolution, which has long been used in the extraction and recovery of gold from ores.[9] This reaction requires a Lewis base ligand (often a halide or pseudohalide) and an oxidant.[10] Common examples of ligand/oxidant couples include Cl^-/NO_3^- (aqua regia), CN^-/O_2, I^-/I_2, and SCN^-/I_2.[10,11] The Lewis base ligand plays two important roles in promoting the oxidation process by (i) lowering the metal's redox potential through chemical adsorption and (ii) complexing and providing stability to the otherwise unstable Au(I) product.[8,12] The oxidation of metallic nanoparticles has also been shown to be particle size-dependent, with smaller particles having more negative redox potentials and being more susceptible to etching than larger particles.[8,12−14] Ivanova and Zamborini, for example, recently reported a difference of ca. 200 mV in the oxidation potentials of Au nanoparticles of 250 (913 ± 19 mV) and 4 nm (734 ± 1 mV) in diameter.[14] Small nanoparticles also tend to be completely dissolved more quickly than large nanoparticles because they are composed of fewer atoms. Together, these factors permit smaller particles to be sometimes preferentially purified out of samples with bimodal size distributions.[12,15]

Henglein performed seminal experiments on the reactivity of metal nanoparticles in solution, and his work provides an excellent foundation for understanding nanoscale oxidation processes.[8] Several examples of the etching of nanoscale Au have involved oxidation by atmospheric O_2 in the presence of a Lewis base. The use of the CN^-/O_2 couple to etch gold nanoparticles was, for example, utilized by the group of Whitesides.[16] Others have reported the oxidation of Au nanoparticles using Cl^-/O_2 or Br^-/O_2 in the presence of tetraalkylammonium cations.[17,18] The use of ambient O_2 as an oxidant, however, is very difficult to control, and the reaction is mechanistically poorly understood.[18] Oxidation of nanoparticles by O_2 can often be problematic, leading to dramatic, unwanted changes in samples over time (i.e., precipitation, increased polydispersity, size change, etc.). These problems have, for example, often been reported for nanoparticle

Received: April 30, 2012
Revised: June 5, 2012

   dx.doi.org/10.1021/jp304157a | J. Phys. Chem. C XXXX, XXX, XXX−XXX

solutions containing cetyltrimethylammonium bromide (CTAB) and tetraoctylammonium bromide (TOAB).[17−20] Tetraalkylammonium and tetraalkylphosphonium cations generally promote oxidation by stabilizing Au(I) oxidation products.[12,20]

Rodriguez-Fernandez et al. recently demonstrated that gold nanoparticles can be oxidized stoichiometrically by Au(III) in the presence of CTAB micelles in water.[12] They employed this oxidation reaction in the sculpting of Au nanorods and nanospheres. A model was proposed that emphasized the role of charged micelles in spatially directing the oxidation of nanoparticles protected by a charged bilayer of CTAB. Their model, in particular, identified nanoparticle curvature as the dominant factor in controlling oxidation by micelles in water. Khanal and Zubarev subsequently demonstrated that the same reaction could be used in the purification of high aspect ratio Au nanorods in water.[15]

The oxidation of Au nanoparticles by Au(III) is of both fundamental and practical importance. This reaction likely plays a key, but poorly understood, role in the reduction of Au(III) precursors to Au(0) nanoparticles, and in galvanic replacement using Au(III).[21,22] Indeed, for several nanoparticle systems, this oxidation reaction appears to compete kinetically with the Au(0)-generating reactions in these processes. In the synthesis of Au nanoparticles stabilized by tetraalkylammonium complexes (including TOAB), for example, Au(0) nanoparticles do not persist in solution until all Au(III) has been exhausted (i.e., been converted to Au(I)).[23,24] The oxidation of Au nanoparticles by Au(III) can be practically employed in (i) sculpting nanoparticles, (ii) dissolution of nanogold templates, (iii) determination of Au content, (iv) removal of ligands from nanoparticles for quantification, (v) size and shape purification of nanoparticles, and (vi) Au recovery. In this context, we report here the rapid, stoichiometric oxidation of gold nanoparticles by organo-soluble, nonmicellar tetraalkylammonium and tetraalkylphosphonium Au(III) complexes in toluene. Nanoparticle oxidation is shown to proceed according to a comproportionation mechanism (also commonly referred to as conproportionation or symproportionation)[12] and generate stable Au(I) complexes of the ammonium and phosphonium cations used. These redox reactions are studied for several organo-soluble nanoparticle systems, and Au nanorods stabilized in toluene are successfully sculpted. Tetraalkylammonium and tetraalkylphosphonium halide complexes are shown to play a key role in stabilizing particles against aggregation during the oxidation process, and a reaction mechanism is proposed. The model proposed here for ion pairs reacting in toluene is notably distinct from the model proposed for micelles reacting with bilayer-protected nanoparticles in aqueous solution.[12] The reduction of Au(I) and Au(III) complexes to Au(0) nanoparticles during regular TEM imaging was also observed. This unwanted reaction likely occurs frequently in laboratories worldwide, particularly in work on Au nanoparticle systems where oxidation is a known problem (i.e., CTAB, TOAB) or where reduction of precursors is incomplete (including mechanistic studies where midreaction TEM sampling is customary). This reaction is undoubtedly responsible for a plethora of misleading or confusing results that have been reported in the literature.

EXPERIMENTAL SECTION

Chemicals and Reagents. Unless otherwise noted, reagents were obtained from Sigma-Aldrich and used as received. Tetraoctylammonium tetrabromoaurate ([TOA][$AuBr_4$]), tetraoctylammonium dibromoaurate ([TOA][$AuBr_2$]), and tetraoctylphosphonium tetrabromoaurate ([TOP][$AuBr_4$]) were prepared according to previously published methods.[25] Tetraoctylammonium tetrachloroaurate ([TOA][$AuCl_4$]) was prepared according to a modified literature approach.[26] In brief, stoichiometric amounts of $HAuCl_4 \cdot 3H_2O$ (0.281 g) and tetraoctylammonium chloride (0.416 g) were codissolved in 100 mL of anhydrous ethanol, and the resulting solution was stirred for 30 min. This solution was stored in a freezer overnight, generating a bright yellow precipitate that was recrystallized, filtered, washed with cold ethanol, and dried under vacuum. Thiol-terminated polystyrene (PS-SH) (155 units, M_n 16 200, PI 1.1) was prepared according to a previously published method.[27,28]

Synthesis of TOAB-Stabilized Nanoparticles. Toluene solutions of [TOA][$AuBr_4$] (1 mL, 10^{-2} M) and TOAB (1 mL, 10^{-2} M) were added to 9 mL of toluene stirring (900 rpm) in a 100 mL round-bottomed flask. An aqueous solution of $NaBH_4$ (0.0038 g in 2 mL) was then added quickly, and stirring was continued for 20 min. The aqueous phase was discarded, and the toluene phase was washed with water (20 mL). The isolated toluene nanoparticle solution was then used immediately to avoid changes induced by prolonged exposure to atmospheric oxygen.

Synthesis of Tetraoctylphosphonium Bromide (TOPB)-Stabilized Nanoparticles. Toluene solutions of [TOP][$AuBr_4$] (1 mL, 10^{-2} M) and TOPB (1 mL, 10^{-2} M) were added to 9 mL of toluene stirring (900 rpm) in a 100 mL round-bottomed flask. An aqueous solution of $NaBH_4$ (0.0038 g in 2 mL) was then added quickly, and stirring was continued for 20 min. The aqueous phase was discarded, and the toluene phase was washed with water (20 mL). The isolated toluene nanoparticle solution was used immediately.

Synthesis of Tetraoctylammonium Chloride (TOAC)-Stabilized Nanoparticles. Toluene solutions of [TOA][$AuCl_4$] (1 mL, 10^{-2} M) and TOAC (1 mL, 10^{-2} M) were added to 9 mL of toluene stirring (900 rpm) in a 100 mL round-bottomed flask. An aqueous solution of $NaBH_4$ (0.0038 g in 2 mL) was then added quickly, and stirring was continued for 20 min. The aqueous phase was discarded, and the toluene phase was washed with water (20 mL). The isolated toluene nanoparticle solution was used immediately.

Synthesis of PS-SH-Stabilized Nanorods. Gold nanorods stabilized in toluene by thiol-terminated polystyrene were produced using a previously published method.[29] CTAB-stabilized Au nanorods were prepared according to the Ag(I)-assisted growth method,[30] as described by Smith et al.,[31] then transferred to toluene through ligand exchange with PS-SH.[29] In brief, a gold seed solution was prepared by adding $NaBH_4$ (600 μL, 0.01 M) to a solution of $HAuCl_4$ (250 μL, 0.01 M) and CTAB (9.75 mL, 0.1 M). This solution was stirred for 2 min and then left undisturbed. A growth solution was prepared by mixing solutions of CTAB (9.5 mL, 0.1 M), $AgNO_3$ (75 μL, 0.01 M), $HAuCl_4$ (500 μL, 0.01 M), and ascorbic acid (55 μL, 0.1 M). After sitting 2 h, 12 μL of the seed solution was added to the growth solution. This mixture was capped, inverted twice gently, and left at 25 °C overnight without stirring, generating CTAB-stabilized Au nanorods. This aqueous nanorod solution was added quickly to 30 mL of a stirring (600 rpm) acetone solution (5 mg/mL) of PS-SH. A sticky pink precipitate formed and was deposited on the magnetic stir bar and the walls of the round-bottomed flask. The acetone/water mix was decanted

dx.doi.org/10.1021/jp304157a | J. Phys. Chem. C XXXX, XXX, XXX−XXX

off. The precipitate was then washed with acetone and water and readily dissolved in toluene. The toluene solution was washed further with water and dried under reduced pressure for storage. Further purification was accomplished through repeated precipitation−centrifugation steps (6000 rpm, 15 min) in 30 mL of dichloromethane (10%) and acetone (90%) mixtures. Purified nanorods were redissolved in 10 mL of toluene.

Synthesis of Thiolate-Protected Nanoparticles. Dodecanethiolate-protected Au nanoparticles were prepared according to a modified Brust−Schiffrin synthesis.[32] In brief, TOAB (1.5 g) dissolved in 80 mL of toluene was stirred with $KAuBr_4$ (0.507 g) dissolved in 25 mL of water until the aqueous phase became colorless. This indicated the complete phase transfer of the $AuBr_4^-$ anion, forming $[TOA][AuBr_4]$ in the organic phase. The aqueous phase was then discarded, and 2 equiv of dodecanethiol (438 μL) were added to the toluene phase. $[TOA][AuBr_2]$ and dodecyl disulfide were generated, leaving a colorless solution.[25] A 25 mL aqueous solution of $NaBH_4$ (0.380 g) was then quickly added, generating a dark nanoparticle solution in the toluene phase. Stirring was continued for 1 h. The aqueous phase was discarded, and the toluene was removed from the nanoparticle solution by rotary evaporation. The solid product was then dispersed in 50 mL of anhydrous ethanol, collected on a glass filtration frit, washed thoroughly with anhydrous ethanol and acetone, and dried under vacuum.

Oxidation of Nanoparticles. Titration experiments to determine the stoichiometry of the oxidation of Au nanoparticles by Au(III) complexes ($[TOA][AuBr_4]$, $[TOA][AuCl_4]$, or $[TOP][AuBr_4]$) were conducted with freshly prepared nanoparticle solutions. Au(III) complexes (10^{-2} M in toluene) were titrated 0.1 equiv at a time (relative to known Au(0) amounts in nanoparticle solutions) into as-prepared nanoparticle solutions. The localized surface plasmon resonance (LSPR) spectra of the nanoparticle solutions were monitored and allowed to stabilize between each addition. TOAB (10 equiv) was added to purified thiolate-protected nanoparticle samples prior to titration with 10^{-2} M $[TOA][AuBr_4]$ in toluene. The kinetics of nanoparticle oxidation were studied by monitoring the disappearance of the LSPR band with the addition of 0.5 equiv of Au(III) complex (relative to Au(0) amounts in nanoparticle solutions) to as-prepared nanoparticle solutions. The sculpting of PS-SH-stabilized nanorods was accomplished by titrating 600 μL of an oxidant solution (200 μL at a time) into 10 mL of an as-prepared nanorod solution in toluene. The oxidant solution was prepared by adding TOAB (1 mL, 10^{-2} M) and $[TOA][AuBr_4]$ (20 μL, 10^{-2} M) to 1 mL of toluene. The LSPR spectra of the nanorod solution was monitored and allowed to stabilize between each addition. Following oxidation, Au nanorod solutions were purified by centrifugation (10 000 rpm) prior to TEM sample preparation.

Instrumentation. Absorbance spectra and kinetic plots were collected using a Cary 5000 UV−visible−near-IR spectrophotometer equipped with a multicell accessory with magnetic stirring. Samples were stirred during the collection of kinetic data. Transmission electron microscopy (TEM) imaging was performed using a Philips CM200 transmission electron microscope. Samples were cast from solution onto 400 mesh carbon-coated Cu grids. Thermogravimetric analysis (TGA) data was collected using a TA Instruments Q500 thermogravimetric analyzer. Au nanoparticle samples (ca. 5 mg) were placed on a Pt pan and heated to 700 °C under N_2. All ^1H NMR spectra were obtained from deuterated toluene solutions using a 400 MHz Varian Mercury solution NMR spectrometer. Raman scattering spectra were collected from solid samples with a Horiba Jobin Yvon LabRAM HR Raman spectrometer using 633 nm laser excitation.

RESULTS AND DISCUSSION

We recently reported that tetraalkylammonium Au complexes are the relevant Au precursors in two-phase Brust−Schiffrin nanoparticle syntheses rather than Au(I) thiolate polymers, as had been previously believed.[25] That work demonstrated the high solution stability of the Au(I) complex $[TOA][AuBr_2]$ and prompted us to prepare both $[TOA][AuBr_2]$ and $[TOA][AuBr_4]$. With these complexes in hand, we soon recognized that $[TOA][AuBr_4]$ readily etches TOAB-stabilized Au nanoparticles in toluene to produce a colorless solution of $[TOA][AuBr_2]$ (vide infra). A TEM image of the TOAB-stabilized nanoparticles that were thus oxidized is shown in Figure 1a. The initial nanoparticles had an average diameter of ca. 6 nm. The stoichiometry of this oxidation was studied by monitoring UV−visible absorption while titrating a freshly prepared TOAB-stabilized nanoparticle solution with a $[TOA][AuBr_4]$ solution 0.1 equiv at a time (Figure 1b). The LSPR of the Au nanoparticles decreased in intensity with each addition. Complete dissolution of the Au nanoparticles occurred when 0.5 equiv of $[TOA][AuBr_4]$ had been added (relative to equiv of Au(0)). The solution was stable and colorless at this point (bottom spectrum Figure 1b), exhibiting neither Au(0) nanoparticle nor Au(III) absorbance. Upon further addition of $[TOA][AuBr_4]$, however, the characteristic Au(III) complex absorbance at 402 nm increased, indicating that it was no longer being consumed and was accumulating in solution. These observations are consistent with the comproportionation of gold according to reaction 1.

$$[TOA][AuBr_4] + 2Au(0) + 2TOAB \rightarrow 3[TOA][AuBr_2] \quad (1)$$

The colorless product of this reaction (after 0.5 eq $[TOA][AuBr_4]$ was added) was confirmed to be $[TOA][AuBr_2]$ by Raman scattering (Figure S1 of the Supporting Information) and ^1H NMR (Figure S2 of the Supporting Information) spectroscopies. The Raman scattering spectrum of the colorless product matches that of $[TOA][AuBr_2]$ synthesized according to a published method,[25] and shows the characteristic 209 cm^{-1} Au−Br stretch of the $AuBr_2^-$ anion.[26] The ^1H NMR spectrum of the colorless product is consistent with that of $[TOA][AuBr_2]$.[25]

Reaction 1 proceeds quickly for these 6 nm nanoparticles at these concentrations. Figure 1c shows a plot of the LSPR decrease with time for the reaction of TOAB-stabilized Au nanoparticles with 0.5 equiv $[TOA][AuBr_4]$. Complete nanoparticle dissolution occurred in less than 5 min, which is a practical time scale for most applications. The stoichiometry for the complete dissolution of particles with $[TOA][AuBr_4]$ was the same for reactions conducted under either ambient air or Ar atmosphere (results not shown). This is consistent with our observations that oxidation of TOAB-stabilized nanoparticles by atmospheric O_2 is much slower (many days) than oxidation by $[TOA][AuBr_4]$. Although nanoscale Au(0) is readily oxidized by $[TOA][AuBr_4]$ in the presence of TOAB, bulk Au(0) is not (clean Au(0) wire does not react appreciably with $[TOA][AuBr_4]$). This remarkable result is consistent with the

dx.doi.org/10.1021/jp304157a | J. Phys. Chem. C XXXX, XXX, XXX−XXX

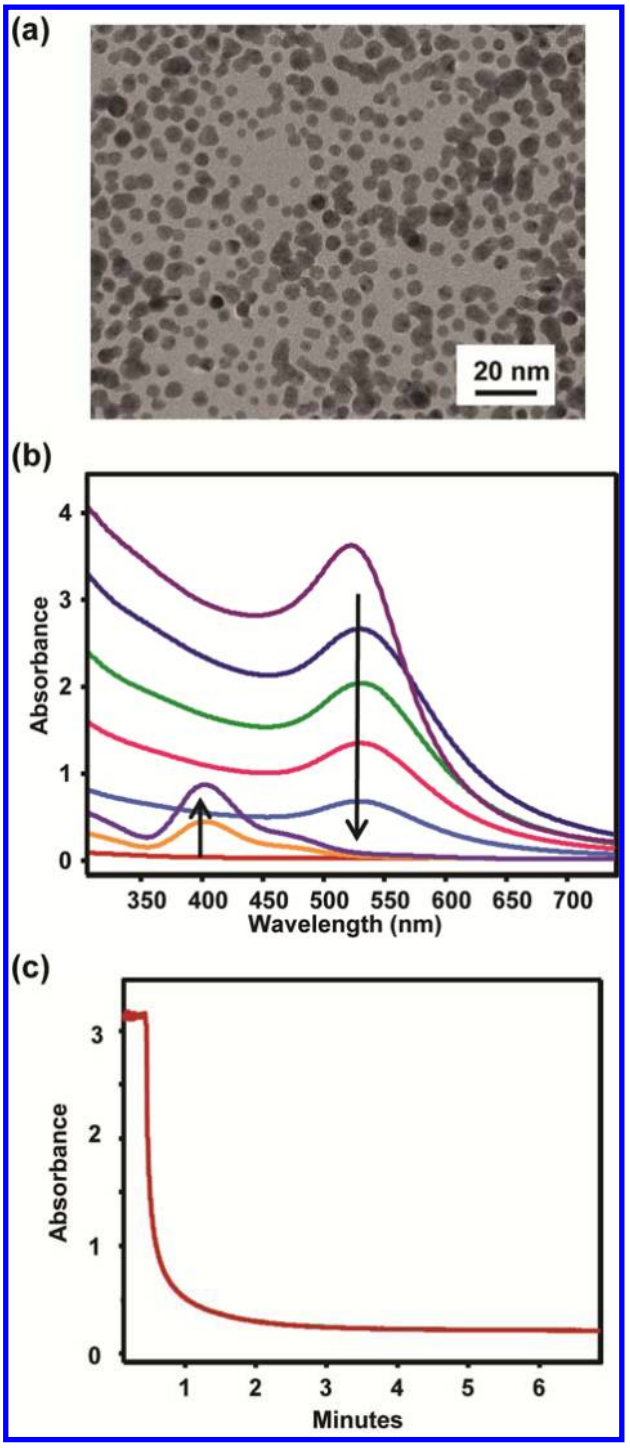

Figure 1. (a) TEM image of TOAB-stabilized Au nanoparticles. (b) UV−visible absorption spectra for the titration of TOAB-stabilized Au nanoparticles (top spectrum) with [TOA][$AuBr_4$] (0.1 equiv at a time). (c) Plot of LSPR (523 nm) decrease with time for the reaction of TOAB-stabilized Au nanoparticles with 0.5 equiv [TOA][$AuBr_4$].

redox potential of Au indeed being dependent on particle size, although we cannot rule out other possible explanations.[8,12−14]

There is a distinct broadening and red shift of the LSPR upon the first addition of [TOA][$AuBr_4$] to TOAB-stabilized nanoparticles (Figure 1b). An increase in the absorbance in the range from 600 to 800 nm is also evident. These spectral changes are consistent with a slight aggregation of the particles as reaction 1 proceeds. A reaction mechanism is proposed in Scheme 1 to account for this aggregation. Electrons are transferred to $AuBr_4^-$ from two Au(0) atoms on the surface of

Scheme 1. Proposed Reaction Mechanism for Comproportionation of Au(0) and Au(III)

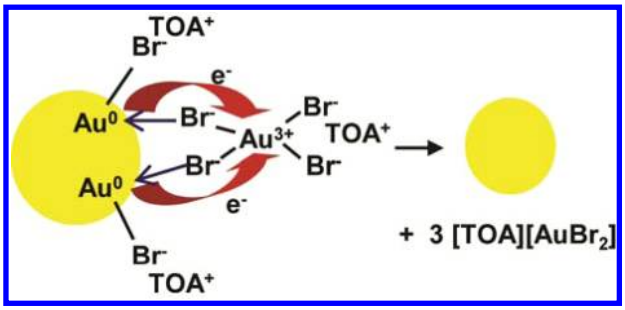

the nanoparticle, and $AuBr_4^-$ transfers two Br^- ions to the resulting surface Au(I). Three [TOA][$AuBr_2$] complexes are thus generated, and two Au atoms and two TOAB capping ligands are lost from the nanoparticle surface as a result. The loss of surface capping ligands with insufficient replacement accounts for the slight extent of nanoparticle aggregation that is observed. To test this hypothesis, we added excess TOAB (10 equiv relative to Au(0)) to as-prepared TOAB-stabilized Au nanoparticles before titrating them with [TOA][$AuBr_4$]. The LSPR of the nanoparticles was monitored and showed no signs of aggregation during the titration (Figure S3 of the Supporting Information). This suggests that the excess TOAB added was sufficient to replace outgoing ligands effectively and stabilize the nanoparticles against aggregation as oxidation progressed.

When the tetraoctylphosphonium cation is substituted for the tetraoctylammonium cation, comproportionation again readily occurs, as expected based on their similar chemical properties. Figure 2 shows UV−visible absorption spectra of

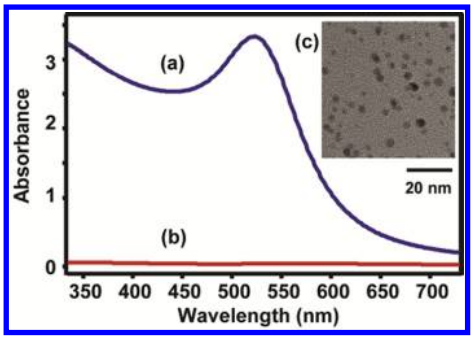

Figure 2. UV−visible absorption spectra of TOPB-stabilized Au nanoparticles (a) before and (b) after the addition of 0.5 equiv of [TOP][$AuBr_4$]. (c) TEM image of TOPB-stabilized Au nanoparticles.

TOPB-stabilized Au nanoparticles before and after the addition of 0.5 equiv [TOP][$AuBr_4$]. Figure 2c shows a representative TEM image of TOPB-stabilized Au nanoparticles that are ca. 4 nm in diameter. These particles are completely oxidized with the addition of 0.5 equiv of [TOP][$AuBr_4$], generating colorless [TOP][$AuBr_2$] according to reaction 2.

$$[TOP][AuBr_4] + 2Au(0) + 2TOPB \rightarrow 3[TOP][AuBr_2] \quad (2)$$

Comproportionation also readily occurs when Br^- is substituted with Cl^- in the oxidant complex ([TOA][$AuCl_4$]) and capping ligand (TOAC) (reaction 3).

dx.doi.org/10.1021/jp304157a | J. Phys. Chem. C XXXX, XXX, XXX−XXX

$$[TOA][AuCl_4] + 2Au(0) + 2TOAC \rightarrow 3[TOA][AuCl_2] \quad (3)$$

Figure 3 shows a representative TEM image of TOAC-stabilized Au nanoparticles (ca. 3 nm), and plots of the LSPR

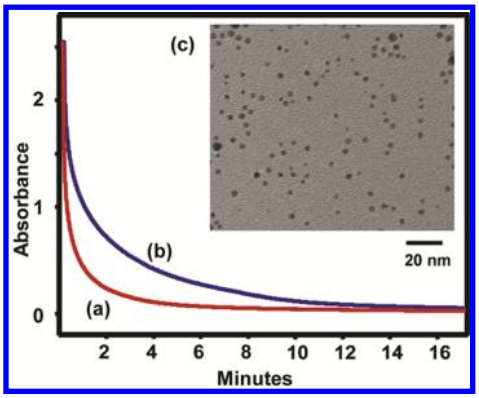

Figure 3. LSPR decrease with time for TOAC-stabilized Au nanoparticles reacting with 0.5 equiv of (a) $[TOA][AuBr_4]$ or (b) $[TOA][AuCl_4]$. (c) TEM image of TOAC-stabilized Au nanoparticles.

decrease with time for the reaction of TOAC-stabilized Au nanoparticles with 0.5 equiv of $[TOA][AuBr_4]$ or $[TOA][AuCl_4]$. Oxidation proceeds more quickly when the Br^- containing complex is employed, as is expected given that Br^- is the stronger Lewis base.

Because the ligands in the nanoparticle systems discussed above do not react with Au(III), quantitative titration is straightforward. In the case of thiolate-protected Au nanoparticles, however, there is a side reaction between free alkylthiol and Au(III) that occurs in addition to the comproportionation reaction (reaction 4).

$$[TOA][AuBr_4] + 2RSH \rightarrow [TOA][AuBr_2] + RSSR + 2HBr \quad (4)$$

This reaction, which we recently reported,[25] consumes Au(III); therefore, greater amounts of the oxidant are required to dissolve unpurified Au(0) nanoparticles completely (i.e., in the presence of free alkylthiol). To confirm that this side reaction occurs, a purified dodecanethiolate-protected Au nanoparticle solution (ca. 2 nm) doped with 3 equiv of free dodecanethiol was titrated with $[TOA][AuBr_4]$. TGA was performed to determine the amount of Au(0) in the solid nanoparticle sample for solution preparation (Figure S4 of the Supporting Information).[33] As expected, a total of 2 equiv of $[TOA][AuBr_4]$ was required to etch completely the Au nanoparticles (Figure 4). 1.5 equiv of $[TOA][AuBr_4]$ was consumed by 3 equiv of free thiol according to reaction 4, and 0.5 equiv of $[TOA][AuBr_4]$ was consumed by 1 equiv of Au(0) according to reaction 1. The ^1H NMR spectrum of the product of this reaction is shown in Figure 4d and confirms the formation of 1.5 equiv of the dodecyl disulfide (α CH_2 proton peak is highlighted).[25] When purified thiolate-protected Au nanoparticles were etched, reaction 4 did not occur and only 0.5 equiv of $[TOA][AuBr_4]$ was required for complete dissolution of 1 equiv of Au(0) nanoparticles (results not shown). Side reactions of this type should be accounted for when employing procedures involving the digestion of nanoparticles in the determination of Au(0) content.

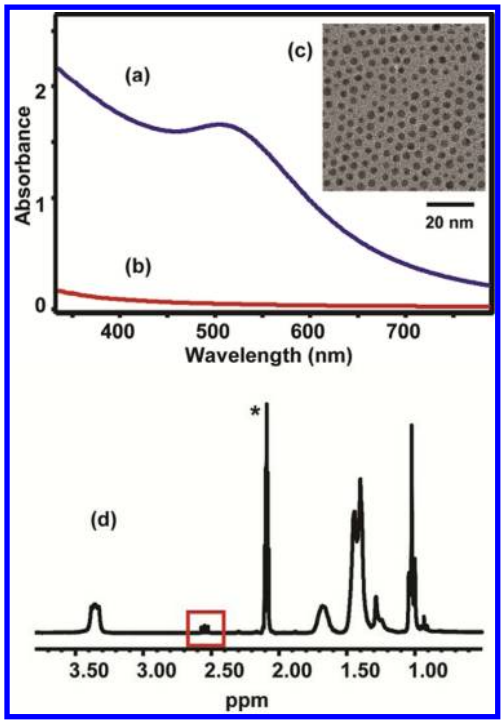

Figure 4. UV−visible absorption spectra of purified dodecanethiolate-stabilized Au nanoparticles, 10 equiv TOAB, and 3 equiv dodecanethiol (a) before and (b) after reaction with 2 equiv $[TOA][AuBr_4]$. (c) TEM image of purified dodecanethiolate-stabilized Au nanoparticles. (d) ^1H NMR spectrum of purified dodecanethiolate-stabilized Au nanoparticles, 10 equiv TOAB, and 3 equiv dodecanethiol after complete reaction with 2 equiv $[TOA][AuBr_4]$. Peak for the α CH_2 protons of dodecyl disulfide is highlighted.

Au(III) complexes can be used to "sculpt" or etch Au(0) nanoparticles systematically in toluene. The sculpting of PS-SH-stabilized Au nanorods by $[TOA][AuBr_4]$ in toluene is demonstrated in Figure 5 as a proof-of-concept. The transverse (540 nm) and longitudinal (794 nm) LSPR bands of the nanorods both lose intensity as $[TOA][AuBr_4]$ is added. There is a clear decrease in the ratio of the longitudinal mode to the transverse mode and a blue shift of the longitudinal mode maximum to 774 nm. These spectral changes are consistent with nanorod shortening due to preferential oxidation at the tips.[12,17] We attribute this preferential oxidation to a greater reactivity of the nanorod tips rather than to an increased collision frequency of micelles with tips, as was reported for CTAB micelle reactions in water.[12] Representative TEM images from before and after oxidation are shown in Figure 5b. Before oxidation, the nanorods are on average ca. 50 nm long and 12 nm wide with an average aspect ratio of ca. 4.2. After oxidation, the nanorods are on average 35 nm long and 10 nm wide with an average aspect ratio of 3.5. It is expected that the sculpting of Au nanoparticles of various other shapes and sizes will also be possible using this approach.

Finally, during the course of this work, we consistently observed that Au(I) and Au(III) complexes were readily reduced to Au(0) nanoparticles under normal TEM imaging conditions. Pure solutions of $[TOA][AuBr_2]$ or $[TOA][AuBr_4]$ (10^{-1} to 10^{-3} M) were dropcast onto carbon-coated Cu grids and imaged at accelerating voltages ranging from 80 to 200 kV to confirm this. In all cases, Au(0) nanoparticles were generated by the reduction of the complexes under the electron beam.

dx.doi.org/10.1021/jp304157a | J. Phys. Chem. C XXXX, XXX, XXX−XXX

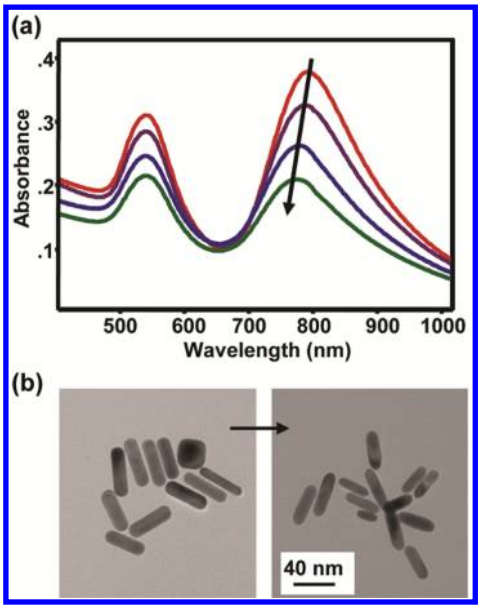

Figure 5. (a) UV−visible absorption spectra for the titration of [TOA][$AuBr_4$] oxidant solution (see Experimental Section) into PS-SH stabilized Au nanorods. (b) TEM images of as-prepared (left) and partially oxidized (right) PS-SH-stabilized Au nanorods.

This unwanted reduction was typically complete before the image was focused and produced large fields of small nanoparticles (ca. 2 nm). Typical images for each metal complex are presented in Figure 6. We also observed reduction

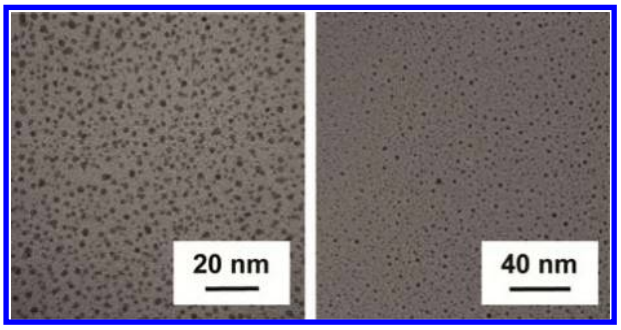

Figure 6. TEM images of Au nanoparticles generated by reduction of [TOA][$AuBr_2$] (left) and [TOA][$AuBr_4$] (right) during TEM measurement.

of Au(I) complexes onto existing nanoparticles (i.e., seeded growth) under the electron beam for samples containing presynthesized nanoparticles. Similar behavior has been previously reported for Au(I)−thiolate complexes.[34−36] It is likely that the reduction of Au(I) and Au(III) complexes during TEM measurement occurs frequently and is undoubtedly responsible for many misleading or confusing results, particularly in work on Au nanoparticle systems where oxidation is a known problem or where reduction of precursors is incomplete. It is thus highly recommended that, in cases where they are likely to be present, all nonzero valent Au complexes be removed from Au nanoparticle samples prior to TEM imaging.

CONCLUSIONS

We have demonstrated the rapid, stoichiometric oxidation of gold nanoparticles by organo-soluble, nonmicellar tetraalkylammonium and tetraalkylphosphonium Au(III) complexes in toluene. Nanoparticle oxidation was shown to proceed according to a comproportionation mechanism and generate stable Au(I) complexes of the ammonium and phosphonium cations used. These reactions were studied for several nanoparticle systems, employing different cations and halides in the oxidant complex. Tetraalkylammonium and tetraalkylphosphonium halide complexes were shown to play a key role in stabilizing particles against aggregation during the oxidation process. A reaction mechanism for comproportionation of Au(0) and Au(III) was proposed. Au(III) oxidant complexes containing Br^- were shown to oxidize nanoparticles more quickly than those containing Cl^-. A side reaction between free thiol and Au(III) was also shown to occur when unpurified thiolate-stabilized nanoparticles were oxidized. As a proof-of-concept, Au nanorods stabilized in toluene were successfully sculpted by Au(III) complexes. Finally, the reduction of nonzero valent Au species during normal TEM imaging was observed. It is expected that awareness of this problem will improve the reliability of TEM imaging of Au nanoparticles.

ASSOCIATED CONTENT

Supporting Information

Raman scattering, ^1H NMR, UV−visible absorption, and TGA data. This material is available free of charge via the Internet at http://pubs.acs.org.

AUTHOR INFORMATION

Corresponding Author

*E-mail: paul.goulet@mail.mcgill.ca, bruce.lennox@mcgill.ca.

Present Address

[†]Department of Chemistry and Biomolecular Science, Clarkson University, Potsdam, NY 13699, USA.

Notes

The authors declare no competing financial interest.

ACKNOWLEDGMENTS

We thank Dr. David Liu for TEM imaging, and Dr. Muriel Corbierre for the synthesis of thiol-terminated polystyrene. The Natural Sciences and Engineering Research Council of Canada (NSERC) and the Centre for Self-Assembled Chemical Structures (CSACS) are gratefully acknowledged for financial support.

REFERENCES

(1) Sardar, R.; Funston, A. M.; Mulvaney, P.; Murray, R. W. *Langmuir* **2009**, *25*, 13840−13851.
(2) Daniel, M.-C.; Astruc, D. *Chem. Rev.* **2004**, *104*, 293−346.
(3) Rosi, N. L.; Mirkin, C. A. *Chem. Rev.* **2005**, *105*, 1547−1562.
(4) Xia, Y.; Xiong, Y.; Lim, B.; Skrabalak, S. E. *Angew. Chem., Int. Ed.* **2008**, *47*, 2−46.
(5) Sperling, R. A.; Rivera Gil, P.; Zhang, F.; Zanella, M.; Parak, W. J. *Chem. Soc. Rev.* **2008**, *37*, 1896−1908.
(6) Chen, M. S.; Goodman, D. W. *Chem. Soc. Rev.* **2008**, *37*, 1860−1870.
(7) Wilson, R. *Chem. Soc. Rev.* **2008**, *37*, 2028−2045.
(8) Henglein, A. *J. Phys. Chem.* **1993**, *97*, 5457−5471.
(9) Marsden, J. O.; House, C. I. *The Chemistry of Gold Extraction*, 2nd ed.; Society for Mining, Metallurgy, and Exploration, Inc.: Littleton, CO, 2006.
(10) Praharaj, S.; Panigrahi, S.; Basu, S.; Pande, S.; Jana, S.; Ghosh, S. K.; Pal, T. *J. Photochem. Photobiol., A* **2007**, *187*, 196−201.
(11) Ukraintsev, V. B.; Matsura, V. A.; Ukraintsev, I. V. *Russ. J. Appl. Chem.* **2005**, *78*, 1555−1558.

(12) Rodriguez-Fernandez, J.; Perez-Juste, J.; Mulvaney, P.; Liz-Marzan, L. M. *J. Phys. Chem. B* **2005**, *109*, 14257−14261.
(13) Plieth, W. J. *Surf. Sci.* **1985**, *156*, 530−535.
(14) Ivanova, O. S.; Zamborini, F. P. *Anal. Chem.* **2010**, *82*, 5844−5850.
(15) Khanal, B. P.; Zubarev, E. R. *J. Am. Chem. Soc.* **2008**, *130*, 12634−+.
(16) Weisbecker, C. S.; Merritt, M. V.; Whitesides, G. M. *Langmuir* **1996**, *12*, 3763−3772.
(17) Tsung, C. K.; Kou, X. S.; Shi, Q. H.; Zhang, J. P.; Yeung, M. H.; Wang, J. F.; Stucky, G. D. *J. Am. Chem. Soc.* **2006**, *128*, 5352−5353.
(18) Dasog, M.; Scott, R. W. J. *Langmuir* **2007**, *23*, 3381−3387.
(19) Aguirre, C. M.; Kaspar, T. R.; Radloff, C.; Halas, N. J. *Nano Lett.* **2003**, *3*, 1707−1711.
(20) Zotti, G.; Vercelli, B.; Berlin, A. *Anal. Chem.* **2008**, *80*, 815−818.
(21) Dey, G. R.; El Omar, A. K.; Jacob, J. A.; Mostafavi, M.; Belloni, J. *J. Phys. Chem. A* **2011**, *115*, 383−391.
(22) Cobley, C. M.; Xia, Y. N. *Mater. Sci. Eng., R.* **2010**, *70*, 44−62.
(23) Abecassis, B.; Testard, F.; Kong, Q.; Francois, B.; Spalla, O. *Langmuir* **2010**, *26*, 13847−13854.
(24) Wang, J.; Boelens, H. F.; Thathagar, M. B.; Rothenberg, G. *ChemPhysChem* **2004**, *5*, 93−98.
(25) Goulet, P. J. G.; Lennox, R. B. *J. Am. Chem. Soc.* **2010**, *132*, 9582−9584.
(26) Braunstein, P.; Clark, J. H. *J. Chem. Soc., Dalton Trans.* **1973**, 1845−1848.
(27) Corbierre, M. K.; Cameron, N. S.; Sutton, M.; Mochrie, S. G. J.; Lurio, L. B.; Rühm, A.; Lennox, R. B. *J. Am. Chem. Soc.* **2001**, *123*, 10411−10412.
(28) Corbierre, M. K.; Cameron, N. S.; Lennox, R. B. *Langmuir* **2004**, *20*, 2867−2873.
(29) Goulet, P. J. G.; Bourret, G. R.; Lennox, R. B. *Langmuir* **2012**, *28*, 2909−2913.
(30) Gou, L. F.; Murphy, C. J. *Chem. Mater.* **2005**, *17*, 3668−3672.
(31) Smith, D. K.; Miller, N. R.; Korgel, B. A. *Langmuir* **2009**, *25*, 9518−9524.
(32) Brust, M.; Walker, M.; Bethell, D.; Schiffrin, D. J.; Whyman, R. *J. Chem. Soc., Chem. Commun.* **1994**, 801−802.
(33) Hostetler, M. J.; et al. *Langmuir* **1998**, *14*, 17−30.
(34) Corbierre, M. K.; Beerens, J.; Lennox, R. B. *Chem. Mater.* **2005**, *17*, 5774−5779.
(35) Kim, J.-U.; Cha, S.-H.; Shin, K.; Jho, J. Y.; Lee, J.-C. *J. Am. Chem. Soc.* **2005**, *127*, 9962−9963.
(36) Corbierre, M. K.; Beerens, J.; Beauvais, J.; Lennox, R. B. *Chem. Mater.* **2006**, *18*, 2628−2631.